



Pristine graphene and graphene oxide induce multi-organ defects in zebrafish (*Danio rerio*) larvae/juvenile: an in vivo study

Bangeppagari Manjunatha¹ · Eunseok Seo² · Sung Ho Park² · Rajesh R. Kundapur³ · Sang Joon Lee^{1,2}

Received: 16 June 2020 / Accepted: 16 February 2021 / Published online: 3 March 2021
© The Author(s), under exclusive licence to Springer-Verlag GmbH, DE part of Springer Nature 2021

Abstract

Graphene-based nanomaterials (GBNs) have been widely used in various fields nowadays. However, they are reported to be highly toxic to some aquatic organisms. However, the multi-organ toxicity caused by pristine graphene (pG) and graphene oxide (GO) to the developing zebrafish (*Danio rerio*) larvae or juvenile and the underlying mechanisms is not fully known. Therefore, in the present study, the effect of pG and GO with environmental concentrations (0, 5, 10, 15, 20, and 25 µg/L of pG; 0, 0.1, 0.2, 0.3, and 0.4 mg/mL of GO) on multi-organ system in developing zebrafish larvae was experimentally assessed. The pG and GO were found to accumulate in the brain tissue that also caused significant changes in the heart beat and survival rate. The sizes of hepatocytes were reduced. Altered axonal integrity, affecting axon length and pattern in “Tg(mbp:eGFP) transgenic lines” was also observed. In addition, the results indicated pathological effects in major organs and with disrupted mitochondrial structure was quite obvious. The pG and GO bioaccumulation leads to multi organ toxicity in zebrafish larvae. In future, the existence of the current study can be extrapolated to other aquatic system in general and in particularly to humans.

Keywords Graphene materials · Zebrafish larvae/juvenile · Brain accumulation · Cardiotoxicity · Hepatotoxicity · Neurotoxicity

Introduction

Although nanotechnology is a novel field, the use of nanoparticles dates back to tenth century BC (Brayner 2008). Advances of nanotechnology make nanomaterial (NM) to be used in various products in our daily life, including medicines, cosmetics,

and allied goods. Because of its environmental release, a significant increase of NM concentration is expected in fresh and marine waters, sediments and soils (Giese et al. 2018). Despite the increasing production and use of NM, their toxic effects on the aquatic environment and human health remain unclear (Khan et al. 2019). Furthermore, toxicological and ecotoxicological data for commercial NM-based products are lacking and there is an increased concern about their toxicological classification and regulation (Bundschuh et al. 2018).

The graphene family contains most attractive NM (Guo and Mei 2014). Graphene-based nanomaterials (GBNs), used in a wide variety of applications, are increasingly introduced into aquatic environments. This kind of situation urgently calls for detailed studies on the toxicity of GBNs to assess its environmental hazard and risk assessment. During the synthesis, application, and disposal processes of GBNs, graphene oxide (GO) is likely introduced into aquatic environment, causing potential environmental risks (Chen et al. 2016; Zhao et al. 2016). The toxicity and potential side effects of graphene on health tissues have been reported (Bianco 2013; Chowdhury et al. 2013b).

In our previous studies, pG and GO were found to be significantly toxic to zebrafish embryos by inducing mortality, apoptosis, delayed hatching, and inhibition of blood formation causing abnormal heartbeat, cardiovascular defect, and retardation of cardiac

Responsible editor: Philippe Garrigues

✉ Sang Joon Lee
sjlee@postech.ac.kr

Bangeppagari Manjunatha
manjubhargav2010@gmail.com

Eunseok Seo
seven@postech.ac.kr

Sung Ho Park
shpark1222@postech.ac.kr

Rajesh R. Kundapur
rajeshkundapur123@gmail.com

¹ Center for Biofluid and Biomimic Research, Pohang University of Science and Technology (POSTECH), Pohang 37673, South Korea

² Department of Mechanical Engineering, Pohang University of Science and Technology (POSTECH), Pohang 37673, South Korea

³ Glorious Exotica Lab, Pune, India

looping (Manjunatha et al. 2018a, b). Moreover, pG not only was harmful to the brain development (Sawosz et al. 2014) but also caused damage to mitochondria and altered hepatocyte ultrastructure in chicken embryos (Szmidt et al. 2016). In addition, in vivo study on the effects of GO was carried out by intentionally injecting it into the body cavity of *Acheta domesticus* (Dziewiecka et al. 2016). As a result, GO increased the level of reactive oxygen species (ROS) within 48 h after the injection. Compared to pG, GO is rich in oxygen-containing groups. Thus, GO is more soluble in water and it can easily match with food chains (Chowdhury et al. 2013a). Evidently, there are several reports on the ill effects of G (graphene) and GO on the environment (Modi et al. 2017; Mu et al. 2017; Zhang et al. 2017). A study of Lim et al. (2016) examined the role of GO in inducing apoptosis and death by activating autophagy. GO is also responsible for evoking the DNA lesion formation, granulomatous inflammation, and growth retardation (Xu et al. 2016). Nanosheets of G and GO were found to induce DNA damage, generate reactive oxygen species (ROS), and activate the base excision repair (BER) signaling pathway in the cells and zebrafish larvae (Akhavan et al. 2012; Lu et al. 2017a). Recently, it was reported that graphene induces different grades of toxicological effects that are dependent on the analyzed organ in *Danio rerio* (Fernandes et al. 2018).

Accordingly, it is essential to study their nanotoxicity and environmental influences. Zebrafish (*Danio rerio*) has been used as a popular vertebrate model for studying the toxicities of a variety of nanomaterials. In toxicological assessments, zebrafish has previously been used as a credible in vivo model to investigate the development and growth, molecular biomarker of oxidative stress, and various molecular pathways related to DNA damage responses (Dai et al. 2014; Ersahin et al. 2015; Lu et al. 2017b). There are a few studies about the toxicity assessment of GBNs on zebrafish development. However, to the best of our knowledge, no study addressed the effect of multi-organ toxicity of pG and GO on zebrafish development.

Therefore, this study was aimed to further investigate the impacts of pG and GO nanomaterials on zebrafish (*Danio rerio*) with focusing on multi-organ toxicity including brain accumulation toxicity, cardiotoxicity, hepatotoxicity, and neurotoxicity. In addition, the in vivo visualization assays employed in this study can provide valuable information for further detailed assessments to be made before releasing them into the environment.

Materials and methods

Ethical statement

All experiments using zebrafish (*Danio rerio*) were performed according to the animal protocol approved by the Animal Care

and Ethics Committee of POSTECH (POSTECH-2019-0059), South Korea.

Characterization of pG and GO

Pristine graphene (pG) monolayer flakes (1 mg/L), to measure the size, thickness, and diameter, were used as described in our earlier study (Manjunatha et al. 2018a). Graphene oxide (GO) nanoparticles' (4 mg/mL) related information was procured from the Graphenea company.

Zebrafish embryo collection

The zebrafish lines, including wild type, Tg(Lfabp:dsRED), and Tg(mbp:eGFP), were obtained from the ZCDM (Zebrafish Center for Disease Modeling), South Korea. Zebrafish embryos were maintained as previously described in Bangeppagari et al. (2019). In this study, "larvae" refer to the hatched animals over 6 days post-fertilization (dpf) and "juvenile" refer to the 30 dpf. A schematic of the experimental design is illustrated in supplementary information.

Exposure of pG and GO to zebrafish larvae

Wild type zebrafish larvae at 6–10 dpf were exposed to pG and GO (0, 5, 10, 15, 20, and 25 µg/L of pG; 0, 0.1, 0.2, 0.3, and 0.4 mg/mL of GO) for toxicological long-term observation in the developmental period. These environmental concentrations were fixed, based on our earlier studies considering the toxicity of pG and GO in zebrafish embryogenesis (Manjunatha et al. 2018b; Manjunatha et al. 2019). In these experiments, each concentration group was treated in triplicate. The larval survival rate was monitored every 24 h and the heart rate in the zebrafish larvae was measured at 8 and 10 dpf. Larvae ($n=10$) used for each group were anesthetized with 0.016% tricaine (Sigma) and their heart beat was counted for 30 s using an inverted microscope (Zeiss Axiovert 200; Zeiss, Germany).

Assessment of post-exposure accumulation of pG and GO in the larvae

The relative accumulation of pG and GO was evaluated by using the fluorescent properties of pG and GO with the aid of a microscopic imaging technique. Firstly, 6-dpf-old zebrafish larvae (10 larvae/well) were transferred into a 24-well plate containing 2-mL fish media and treated with pG and GO, respectively, and allowed to grow for further studies. After 10 dpf, the control and treated live zebrafish larvae were stained with acridine orange (AO) and the detailed procedure was described as previous study in Manjunatha et al. (2018b). Briefly, the larvae were then rinsed twice in phosphate-buffered saline (PBS), to remove and reduce any pG and

GO particles that might remain on surfaces of the larvae. Therefore, the larvae were anesthetized in tricaine (0.016%). The relative fluorescence intensity in the larval head (mainly brain) was visualized with a confocal microscopy (Leica TCS SP5, Germany). The experiment was repeated on three independent zebrafish clutches ($n = 3$).

Post-exposure hepatotoxicity assessment

Transgenic zebrafish Tg(Lfabp:dsRED) larvae were exposed to pG and GO for 6–10 dpf. Optical images of the liver GFP/RFP fluorescence of larvae were captured using a confocal microscopy (Leica TCS SP5, Germany) attached with GFP/RFP filters. For consistent comparison, all photographs were taken under the same exposure time with a fixed aperture. Ten larvae were randomly selected from each dosage group for images. Swimming larvae were anesthetized in tricaine (0.016%) prior to photographing. ImageJ software was used to monitor deformation of the liver.

Post-exposure neurotoxicity assessment

After exposure of pG and GO to transgenic zebrafish Tg(mbp:eGFP), larvae were treated with pG and GO for 6–10 dpf. Thereafter, then, neuron development and damage were assessed by ImageJ software. All zebrafish larvae were examined with a confocal microscopy (Leica TCS SP5, Germany).

Post-exposure histopathological assessment

After the exposure to pG and GO, the larval zebrafishes were fixed by using 4% paraformaldehyde. The fixed larvae were embedded in paraffin, sectioned, and stained with hematoxylin and eosin. Eventually, for each concentration condition, 10 larvae/juvenile (30 dpf) were tested for histopathological analysis. Slides were analyzed by using a CCD camera (QIMAGINGQ42286, Canada).

Transmission electron microscopy analysis of brain tissue

The control and treated zebrafish larvae (10 dpf) were randomly sampled, euthanized, and fixed overnight. At first, the brain tissues were pre-fixed in 2% paraformaldehyde and 2% glutaraldehyde solution, diced into 0.05 M sodium cacodylate buffer (pH 7.2) overnight, and then post-fixed in 1% osmium tetroxide buffer at 4 °C for 2 h. Then, the test samples were dried using a graded series of ethanol and then further dehydrated in propylene oxide and epoxy resin (Spurr's). Ultrathin sections (60–80 nm) of the brain tissues were made using a Jeol JEM-1011 instrument (Jeol, Tokyo, Japan), and collected on formvar-coated grids. They were then counterstained with 2% uranyl acetate and Reynolds' lead citrate (MT-X, RMC, Tucson, AZ, USA). Each sample was observed by a TEM (Jeol JEM-1011) at 80 kV to check the brain damage and analyze inflammation indexes.

Statistical analysis

Statistical analysis was performed using the GraphPad Prism5 (GraphPad Software Inc., USA). All data were represented as mean \pm S.D. The two-tailed ANOVA test was employed to evaluate the statistical variances in biological limits between each groups. Differences were considered as significant when $*p < 0.0001$.

Results

Larval toxicity induced by pG and GO

The survival rates of zebrafish larvae after treating pG and GO nanomaterials are shown in Fig. 1a and 1b. For the exposure cases of lower concentration groups, the survival rates do not show significant differences from the control group. However, the survival rates were found to be decreased in 20 and 25 $\mu\text{g/L}$ of pG and 0.4 mg/L of GO treated groups at 10 dpf. The

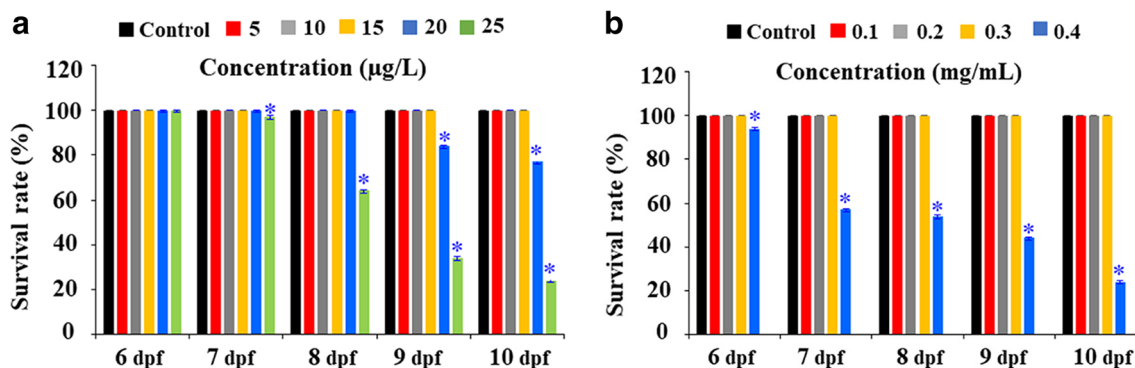


Fig. 1 Survival rate assessment of pG- and GO-induced toxicity in zebrafish larvae during 6–10 dpf. The survival rates of zebrafish larvae are significantly decreased by (a) pG and (b) GO treatment. $n = 10$, each value represent mean \pm S.D. with significance level $*p < 0.0001$

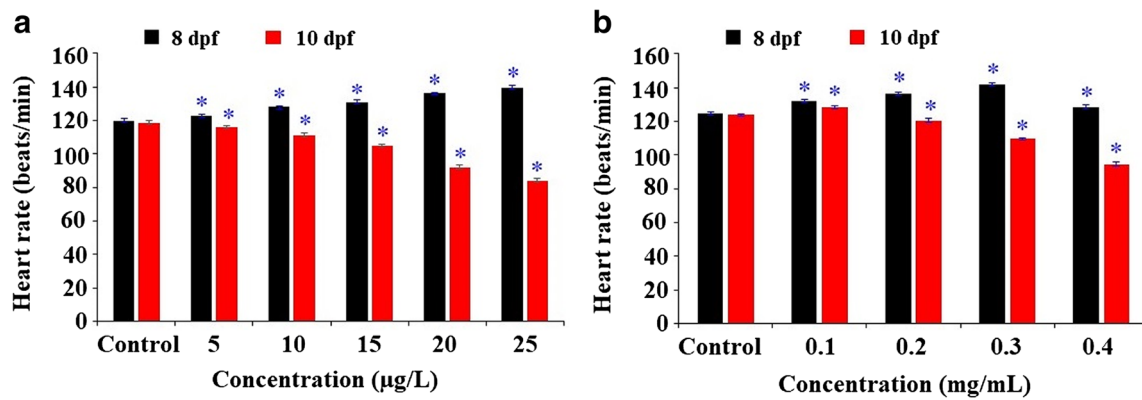


Fig. 2 Heart rate assessment. pG and GO caused heart rate variations in zebrafish larvae ($n = 10$) at 8 and 10 dpf. The heart rates were significantly increased by the treatment of (a) pG and (b) GO at 8 and 10 dpf, respectively; each value represents mean \pm S.D. with significance level $*p < 0.0001$

survival rates of the larvae exposed to PG and GO exhibit significant variations in a time-dependent manner (Fig. 1a and b). Similarly, the heart rates were also significantly increased at 8 dpf and decreased at 10 dpf in post-exposure groups (Fig. 2a and b).

Post-exposure accumulation of pG and GO in the larval body

The accumulation of pG and GO in a respective treated groups increased in a dose-dependent manner. The larvae in the control group were normal fluorescence in the head region, whereas the pG- and GO-treated groups exhibited high fluorescence which is evident in the Fig. 3. This indicates that the brain accumulation toxicity is generated by the presence of pG and GO in zebrafish larvae. Similar results are shown in the histological analysis. The heads of the control group zebrafishes have a normal cell structure (Fig. 6a), while the pG- and GO-treated groups exhibit apoptosis in the brain and degeneration in the eye and brain regions (Fig. 6b and c). Thus, the present results imply that exposed to pG and GO

can cause brain damage in zebrafish larvae due to the effects of accumulation toxicity.

Hepatotoxicity caused by pG and GO

Both treatments of pG and GO induced hepatic malformation in zebrafish larvae which was evident through liver degeneration and hepatotrophya compared to the control larvae (Fig. 4a and b). The liver size was degenerated in a dose-dependent manner (Fig. 4). As seen in Fig. 4c and d, the liver size were significantly reduced to $79.2 \pm 0.5 \%$ for pG (25 $\mu\text{g/L}$) and $164.8 \pm 0.4 \%$ for GO (0.4 mg/mL), respectively, compared to the control larvae (237.9 ± 0.2). Similarly, histological results shows that the liver of the control group zebrafish has a normal cell architecture and tight cell contact (Fig. 6a), while the pG- and GO-treated groups are observed to have loose cell-to-cell contact with asymmetrical structure and tiny vacuoles (Fig. 6b and c). Taken together, the present results indicate that exposed to pG and GO can cause liver degradation in zebrafish larvae.

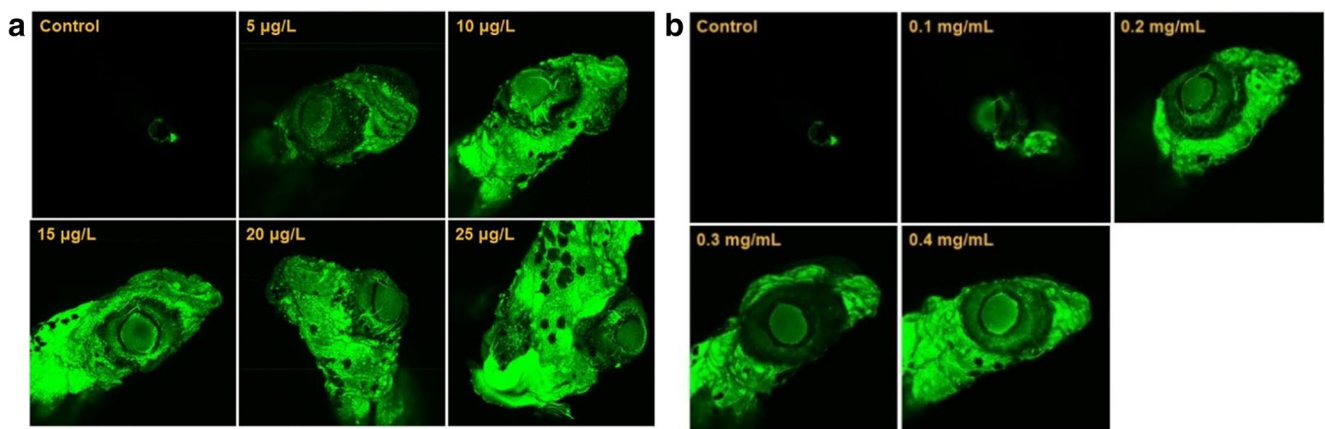


Fig. 3 A visualization of accumulation of pG and GO in zebrafish larvae at 10dpf. **a** pG-treated group showing high fluorescence. **b** GO-treated groups exhibiting high fluorescence. A relatively lesser fluorescence was evident in the respective control groups

Neurotoxicity induced by pG and GO

The confocal microscopic observation of treated group revealed the neuronal damage compared to the control group (Fig. 5). The Tg(mbp:eGFP) transgenic zebrafish lines show an inhibitory effect on the length of axons. Moreover, the axons show structural changes (indicates white arrow) in all pG- and GO-treated groups, especially for the highest concentration conditions of pG (25 $\mu\text{g/L}$) and GO (0.4 mg/mL) (Fig. 5a and b). As seen in Fig. 5c and d, the length of axons significantly decreased to $15.6 \pm 0.09\%$ for pG (25 $\mu\text{g/L}$) and $19.8 \pm 0.4\%$ for GO (0.4 mg/mL) compared to the control larvae (75.8 ± 0.2). Correspondingly, histological images show that the notochord of the control group zebrafish has a normal structure (Fig. 6a), while that in the pG- and GO-treated groups was injured (Fig. 6b and c). Taken together, these results indicate that pG and GO can impair the nervous system by causing neuron damage in zebrafish model.

Histopathological analysis of zebrafish larvae upon pG and GO treatment

The pG- and GO-treated zebrafish larvae exhibit histopathological changes compared to the control group (Fig. 6a, b, and

c). The treated larvae have loose cell-to-cell contacts and large vacuoles in the hepatocytes. They also exhibit alterations in muscle fibers, destroyed gill arches, damages in heart tissue and pancreas, injured notochord, and hyperemia. In addition, the larvae exposed to pG (25 $\mu\text{g/L}$) and GO (0.4 mg/mL) show reduced cell density in the brain region, apoptosis in the brain, degeneration in the brain and eye regions, and thin intestinal walls, frayed gut villi, and widespread cell lysis in the intestines, as shown in Fig. 6b and c with respective letters and colored arrows.

Transmission electron microscopy analysis of brain tissue

Brain cells were observed to have normal architecture in the control zebrafish larvae (Fig. 7a), while abnormal cells with sparse arrangement and pG and GO agglomerates (electron-dense irregular structures) are observed in the treated zebrafish brain tissues. TEM images show that the pG and GO agglomerates are adhered onto the brain cells and internalized in zebrafish larvae (Fig. 7b and c). Some electron-dense irregular thin lines were surrounded by a regular amorphous area in the treated larvae. In addition, the examined brain ultrastructure

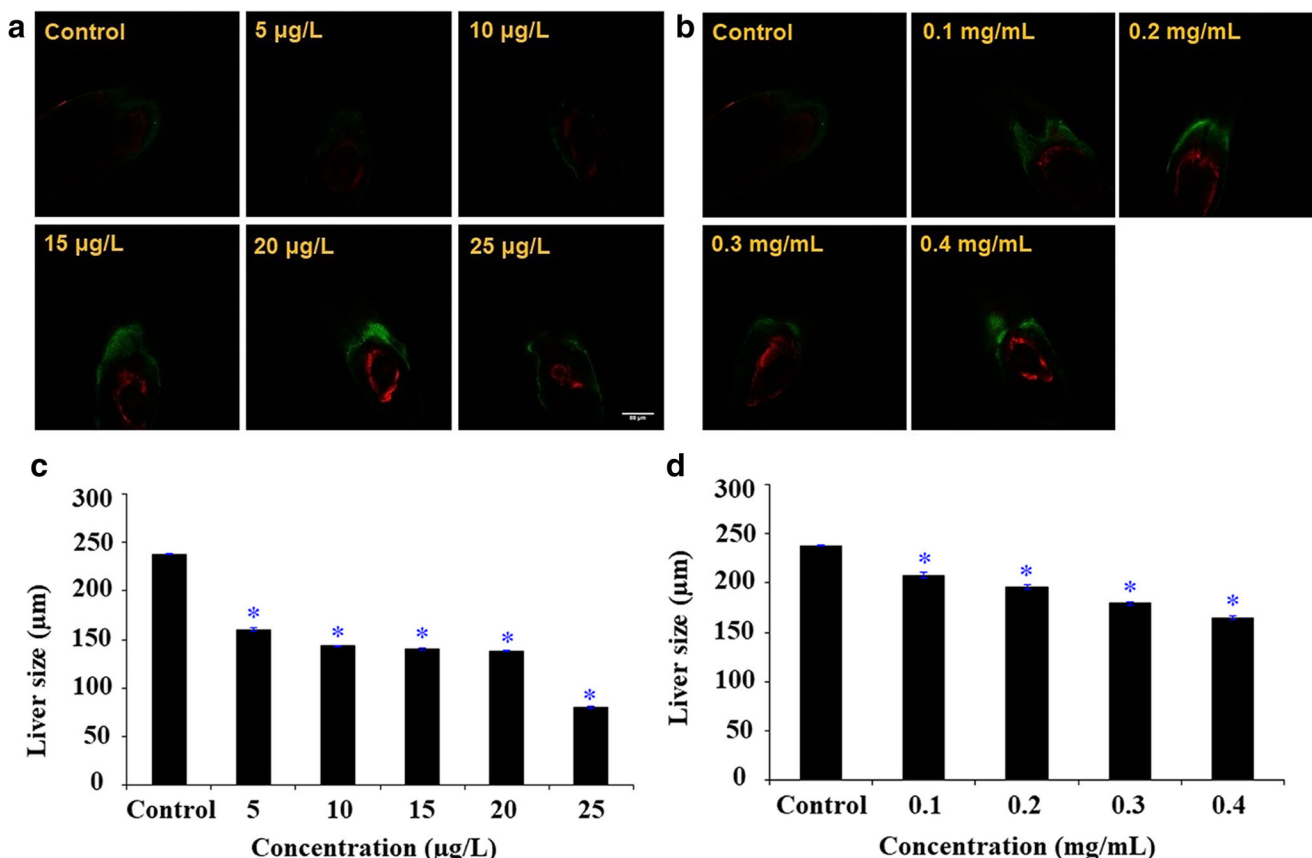


Fig. 4 Hepatotoxicity assessment in pG- and GO-induced zebrafish larvae ($n = 10$). The 10-dpf-old larvae showing degradation of liver tissue, hepatatrophia, and retention upon exposure to (a) pG and (b)

GO. Scale bar denotes 88 μm . Variations in liver size were evident in the treated groups (c) pG and (d) GO. Each value represents mean \pm S.D. with significance level $*p < 0.0001$

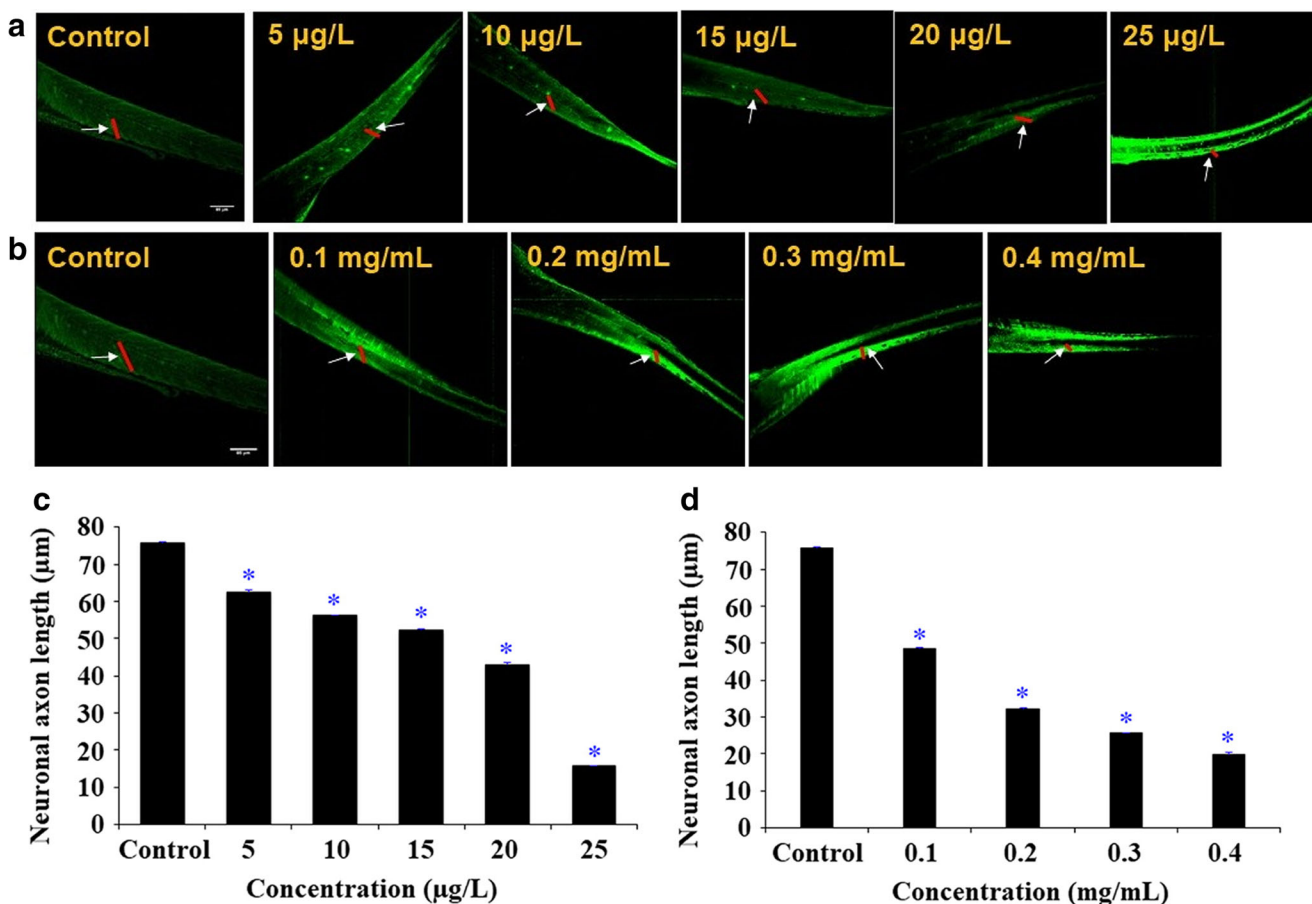


Fig. 5 Neurotoxicity assessment. The pG- and GO-induced neurological defects in 10-dpf-old zebrafish larvae ($n = 10$). The axonal integrity was severely disrupted by pG (a) and by GO (b) causing alteration in axon length with different concentrations especially in Tg (mbp:eGFP)

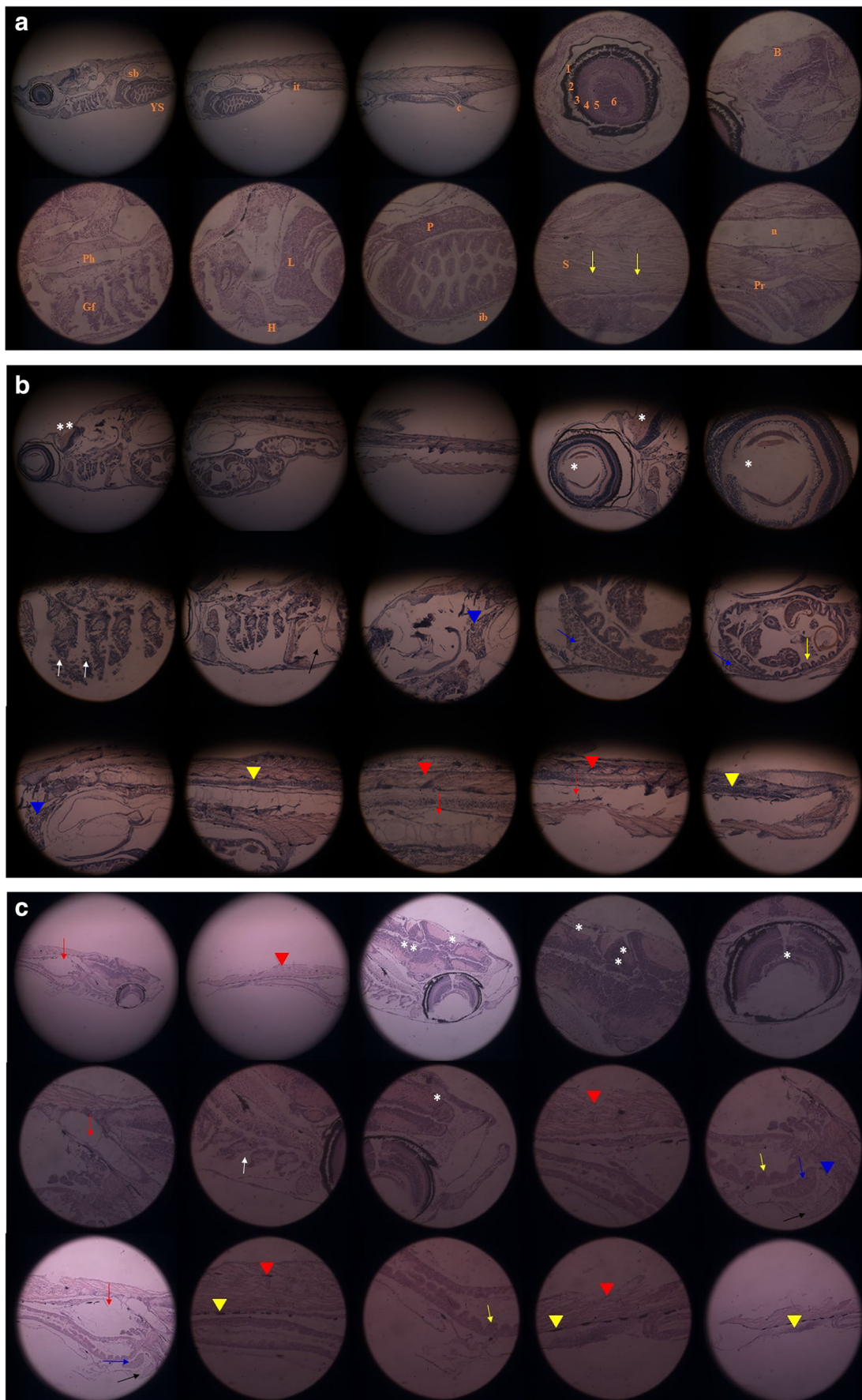
transgenic zebrafish lines. Arrow indicates axonal pattern reduction. Scale bar denotes 85 µm. Variations in axonal length upon exposure to pG (c) and GO (d) were also represented in bar diagram. Each value represents mean ± S.D. with significance level $*p < 0.0001$

indicates some cellular alterations in the pG- and GO-treated larvae. In all graphene-treatment groups, some atypical ultra-structures, such as the increase in the number of vacuoles, blood vessels containing leukocytes, disrupted mitochondria, were observed.

Discussion

Studies on GBNs (pG, GO, rGO, GQDs, and Gr nanoribbons) reported that single or few-layered structures of GBNs are capable of inducing adverse effects in cell lines and animal models (Chong et al. 2014; Jasim et al. 2016). However, GBNs have been widely used in various fields due to rapid increase in production and applications. Thus, the inevitable release of GBNs into water and soil environments poses potential health and ecosystem risks (He et al. 2017). GBNs, one of the most prominently used derivatives of graphene, used in DNA sequencing, drug delivery cargos, and water treatment, their potential toxicity, has not been investigated in detail (Bussy et al. 2015).

Fig. 6 Assessment of histopathological effect of pG and GO. ▶ Histopathological images of 30-dpf-old zebrafish larvae are showed (a) control group; the number represents (1) pigment epithelium; (2) photoreceptor cell layer; (3) inner nuclear layer; (4) inner plexiform layer; (5) ganglion cell layer; and (6) lens. Similarly, letters represent to Ph pharynx; H heart; Gf gill filament; YS yolk Sac; B brain; L liver; P pancreas; S somite; sb swim bladder; ib intestinal bulb; it intestinal track; c cloaca; n notochord; and Pr pronephric duct. Yellow arrow represents normal morphology of muscle fibers. b Histopathological images of pG (25 µg/L) exposed zebrafish larvae at 30 dpf. * refers to degeneration in the eye and in brain regions; whereas ** represents apoptosis in the brain; infected gill chamber (white arrow); damaged heart tissue (black arrow); thin intestinal walls and frayed gut villi (yellow arrow); loose cell-to-cell contacts and large vacuoles in the liver (blue arrow); damaged pancreas with large vacuoles (blue arrowhead); altered muscle fibers (red arrowhead); injured notochord (red arrow); and hyperemia (yellow arrowhead). c Histopathological images of 30-dpf-old zebrafish larvae exposed to GO (0.4 mg/mL). Similarly, * indicates degeneration in the eye and brain regions; ** indicates apoptosis in the brain; destroyed gill chamber (white arrow); thin intestinal walls and frayed gut villi (yellow arrow); loose cell-to-cell contacts and large vacuoles in liver (blue arrow); damaged heart tissue (black arrow); damaged pancreas with large vacuoles (blue arrowhead); altered muscle fibers (red arrowhead); injured notochord (red arrow); and hyperemia (yellow arrowhead)



In the present study, the direct exposure to pG and GO was found to decrease survival rate in a time dependent manner (Fig. 1). The heart rate of zebrafish larvae has significant variations according to the concentration of the exposed pG and GO (Fig. 2). This is well agreed with the earlier studies on zebrafish embryos (Zhang et al. 2017; Manjunatha et al. 2018a; Manjunatha et al. 2019). Furthermore, it also supports the findings of Li et al. (2014) where the toxic effects of graphene nanoparticles (GNP) and graphene-TiO₂ nanoparticle composites (GNP-TiO₂) on the mortality larvae of Japanese medaka fish (*Oryzias latipes*) were studied.

The brain is an important organ for biological behaviors and cognition (Zhao et al. 2015). In the current study, the pG- and GO-induced accumulation toxicity in the head region is largely increased in a dose-dependent manner, as illustrated in Fig. 3. The toxic effects of pG and GO are almost similar; the number of apoptotic cells for both cases were increased as the concentration increases (Manjunatha et al. 2018b; Manjunatha et al. 2019). Similarly, previous studies reported that GO could infiltrate the brains of zebrafish larvae (Ren et al. 2016; Zhang et al. 2017). However, Sun et al. (2019) reported that adult zebrafishes were more tolerant to GO in the range of 0.01–1 mg/L than larvae, and GO could not easily infiltrate the brains of adult zebrafishes due to their strong blood-brain barrier. As a result, zebrafish brain mitochondrial membrane potential was not changed significantly between the control and GO-exposed groups. In addition, the cell junctions were tight, and the nuclei were clear. However, some other cell junctions were not tight, and the nuclei of some cells were distorted. Genes and proteins associated with the brain-blood barrier, such as claudin19 and claudin k, were down-regulated in both the transcriptome and proteome. The decrease in claudin implied the dysfunction of the brain-blood barrier in zebrafish (Zhang et al. 2012; van Leeuwen et al. 2018). Thus, no death or malformation was induced by GO in adult zebrafishes. Given the critical role of brain in biological behaviors and cognition, the molecular responses of zebrafish brain to GO at nonlethal concentrations deserve further study.

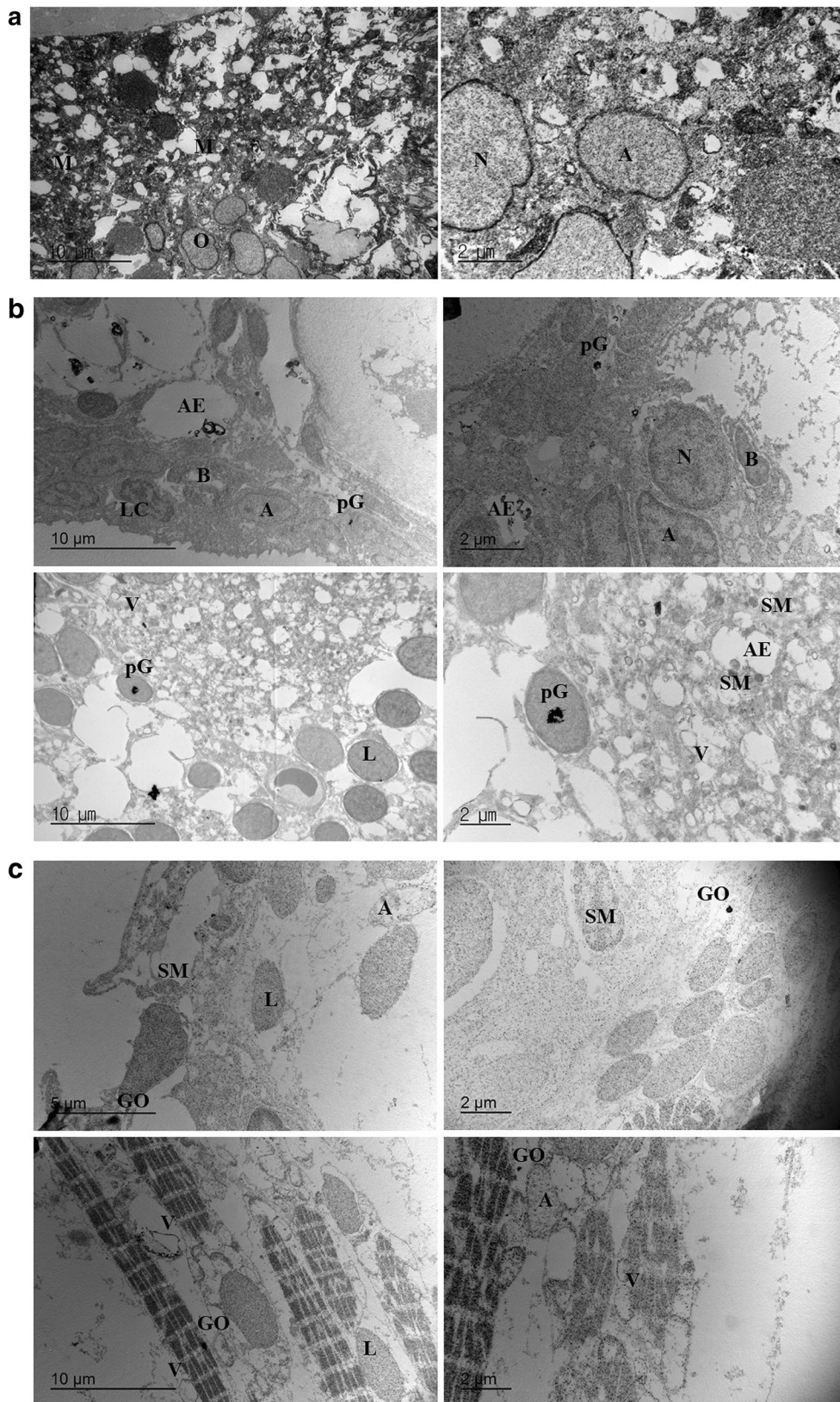
Besides the heart defects induced by exposure of pG and GO, the degradation of liver tissues and hepatatropia are also accompanied with hepatocyte damage (Figs. 4 and 6). Generally, the primary morphogenesis of zebrafish liver begins at the onset of 48 hpf and completes by 72 hpf (He et al. 2013). Interestingly, the liver of zebrafish resembles mammals in terms of anatomy, organization, and function. In recent years, zebrafish emerged as a model to investigate the human diseases like histopathology of cholestasis, fatty liver, and neoplasia (Vliegenthart et al. 2014). The cytochrome 450 (CYP) enzyme family found in hepatocytes are the major part of interest as they are responsible for the initial phase of xenobiotic degradation, drug metabolism, and prodrug activation (Anzenbacher and Anzenbacherová 2001). In view of

this, it was previously reported that diamond nanoparticles (DN), graphene oxide (GO), or graphite nanoparticles (GN) had influence on three isoforms of cytochrome P450 (CYP) enzymes expressed in the liver: CYP1A2, CYP2D6, and CYP3A4. These three nanostructures interact with the CYP enzymes and inhibit their catalytic activity in microsomal-based models. CYP was found to be under expressed in HepG2 and HepaRG cell lines. Among the three nanostructures, GO has the most significant influence on the enzymes, while DN is the most inert (Strojny et al. 2018). In addition, DN, GO, or GN remain within an organism after the administration and they have a tendency to be transported and stored in the liver tissues (Kurantowicz et al. 2015). Tabish et al. (2018) also reported that graphene nanopores (GNPs) induced oxidative stress in the liver of rats. However, there is no significant work on the hepatotoxicity triggered by GBNs in aquatic models available.

In this study, the neurotoxicity of pG and GO on zebrafish was evaluated by using transgenesis and immunofluorescence analyses (Fig. 5). The development of axon is a time-effective means to assess the neurotoxicity screening (Kanungo et al. 2011). The present results confirm that the exposure to pG and GO reduces the axon length and disturbs the axon pattern in zebrafish larvae. Currently, there are limited studies available on the dynamic behaviors of GBNs and neurons. Indeed, those nanomaterials significantly affect the branching and synapses of neurites during differentiation of stem cell to neurons (Defterali et al. 2016a, b). The changes appeared in the differentiation of human-induced pluripotent stem cells into multiple somatic cell lineages similarly shown in Gr-treated samples (Sánchez-González et al. 2018; Saburi et al. 2019). The present results verify that the exposure of pG and GO can indeed disrupt the axonal integrity via impaired axon length and axon pattern.

To better understand, the changes in the structures of cells and tissues in response to toxic pollutants were evaluated by histopathological examination (Meyers and Hendricks 1982), which has been used as an indicator for assessing the aquatic environment (Osterauer et al. 2010). The histopathological examination of the present study shows morphological changes in liver cells, altered muscle fibers, destroyed gill arches, damaged heart tissues, injured notochord, damaged pancreas, and hyperemia. In addition, other alterations such as reduced cellularity and apoptosis in the brain, degeneration in the brain

Fig. 7 TEM analysis of zebrafish larval brain tissue. Images of ultrastructures of brain tissue (a) control group, (b) pG-treated group (25 µg/L), and (c) GO-treated group (0.4 mg/mL) (N nuclei of nerve cells, O nuclei of oligodendroglia, A nuclei of astrocytes, M mitochondria, SM swollen mitochondria, L lysosome, AE amorphous area, V vacuoles, pG graphene-like agglomerates, GO graphene oxide-like agglomerates, LC leukocytes, B blood capillary vessels). Scale bars: 10 µm, 2 µm, 10 µm, 2 µm, 10 µm, 2 µm, 5 µm, 2 µm, 10 µm, 2 µm, from the top to the bottom, respectively



and eye regions, thin intestinal walls, frayed gut villi, and widespread cell lysis are identified in the intestines of larval zebrafish groups exposed to pG (25 µg/L) and GO (0.4 mg/mL) groups, as shown in Fig. 6a, b, and c. Similarly, a previous *in vivo* study reported damage in the main organs of rats (liver, kidney, lungs, heart, brain, and testis) but fast clearance of graphene nanopores (GNPs) through kidney (Tabish et al. 2018). In addition, Souza et al. (2017) demonstrated the organ-specific effects of GO and significant alteration of gills and liver by chronic exposure. Hence, the changes observed in the histopathological examination for the treated larvae further support the abnormalities in the other endpoints studies.

The effects of pG and GO on the brain were examined with special emphasis on their potential localization in the ultrastructures of brain tissues. Morphological variations were observed by TEM analysis. In the present study, we identified the formation of pG and GO agglomerates, some electron-dense irregular thin lines, cellular alterations, atypical ultrastructures, an increase in number of vacuoles, and blood vessels with leukocytes. In addition, mitochondria are partially disrupted in the pG- and GO-treated larvae, compared with the control group (Fig. 7a, b, and c). The brain and intestinal tissues of zebrafish larvae contain GO of 0.01–1.0 µg/L concentration, appeared as dark dots. Despite agglomeration, these observations indicate that GO of ultralow concentration can penetrate the cell membrane and can be accumulated in the target organs (Ren et al. 2016). Although gills in adult zebrafish are the main absorption sites, the accumulation of GBNs may occur in the liver, brain, intestine, and other organs of the body (Lu et al. 2017a, b). Therefore, we hypothesize that such carbon nanomaterials play a key role in their potential for absorption across the target organs. However, highly organized organisms may interact with nanomaterials differently, compared to isolated cells or tissues via cooperation between the cells, tissues, and organs. Moreover, the metabolic environment in the body may interact with chemical groups exposed to the surface of graphene and modify the state of graphene, including agglomeration (Sawosz et al. 2014). Compared to embryos, the use of zebrafish larvae in the evaluation of GBNs toxicity is not fully understood. Moreover, the spatiotemporal mechanism of “miracle materials” pG and GO was explored for the first time in multi-organs of zebrafish model. Even, with these limitations, in addition, we can conclude that further studies are needed on zebrafish larvae before using zebrafish larval model as a reference in the evaluation of GBN toxicity under aquatic environment.

Conclusion

The present study was aimed to assess the *in vivo* interactions of relatively new derivatives of pG and GO (GBNs) exposure and resultant multi-organ toxicity in zebrafish as a model.

Based on the toxicological outcomes obtained in this study, the exposure of pG and GO was found to induce multi-organ toxicity in zebrafish larvae or juvenile, including degeneration in brain and cardiac functions, hepatic damage, and neural impairment. This implies that pG and GO can induce multi-organ toxicity in zebrafish, including the brain, cardio, hepato, and neurotoxicity. In the strict sense, the actual toxicological mechanisms of the zebrafish multi-organ toxicity induced by pG and GO are unclear yet. Further studies, such as correlation analyses on untargeted and high-throughput genes, proteins, metabolites, and other biological endpoints, are required to elucidate the nanotoxicological mechanisms. It will provide basic information for comprehensive understanding on the effect of GBN administration on the target organisms. Furthermore, *in vivo* studies for different animal models are necessary to clarify the toxicity level of different GBN types and to estimate the effects of their concentrations on biomedical applications and environmental hazard.

Supplementary Information The online version contains supplementary material available at <https://doi.org/10.1007/s11356-021-13058-7>.

Author contribution Bangeppagari Manjunatha: investigation, visualization, conceptualization, data curation, methodology, validation, formal analysis, writing - original draft, writing - review and editing, funding acquisition. Eunseok Seo: TEM analysis. Sung Ho Park: zebrafish sources. Rajesh R. Kundapur: formal analysis. Sang Joon Lee: project administration, writing - review and editing, funding acquisition. All authors read and approved the final manuscript.

Funding This study was financially supported by the Korea Research Fellowship (Brain Pool Program) through the National Research Foundation of Korea (NRF) funded by the Ministry of Science and ICT (grant no. 2016H1D3A1938252).

Data availability The obtained and analyzed data of this study are included in this article and available from the corresponding author on reasonable request.

Declarations

Ethics approval and consent to participate All experiments using zebrafish were performed according to the animal protocol approved by the Animal Care and Ethics Committee from POSTECH (POSTECH-2019-0059), South Korea.

Consent for publication Not applicable to this manuscript.

Competing interests The authors declare no competing interests.

References

- Akhavan O, Ghaderi E, Akhavan A (2012) Size-dependent genotoxicity of graphene nanoplatelets in human stem cells. *Biomaterials* 33: 8017–8025

- Anzenbacher P, Anzenbacherová E (2001) Cytochromes P450 and metabolism of xenobiotics. *Cell Mol Life Sci* 58:737–747
- Bangeppagari M, Park SH, Kundapur RR, Lee SJ (2019) Graphene oxide induces cardiovascular defects in developing zebrafish (*Danio rerio*) embryo model: *in-vivo* toxicity assessment. *Sci Total Environ* 673:810–820
- Bianco A (2013) Graphene: safe or toxic? The two faces of the medal. *Angew Chem Int Ed* 52:4986–4997
- Brayner R (2008) The toxicological impact of nanoparticles. *Nano Today* 3:48–55
- Bundschuh M, Filser J, Luderwald S, Mckee MS, Metrevelis G, Schaumann GE, Schulz R, Wagner S (2018) Nanoparticles in the environment: where do we come from, where do we go to? *Environ Sci Eur* 30:1–17
- Bussy C, Jasim D, Lozano N, Terry D, Kostarelos K (2015) The current graphene safety landscape – a literature mining exercise. *Nanoscale* 7:6432–6435
- Chen YM, Hu XG, Sun J, Zhou QX (2016) Specific nanotoxicity of graphene oxide during zebrafish embryogenesis. *Nanotoxicology* 10:45–52
- Chong Y, Ma Y, Shen H, Tu X, Zhou X, Xu J, Dai J, Fan S, Zhang Z (2014) The *in vitro* and *in vivo* toxicity of graphene quantum dots. *Biomaterials* 35:5041–5048
- Chowdhury I, Duch MC, Mansukhani ND, Hersam MC, Bouchard D (2013a) Colloidal properties and stability of graphene oxide nanomaterials in the aquatic environment. *Environ Sci Technol* 47:6288–6296
- Chowdhury SM, Lalwani G, Zhang K, Yang JY, Neville K, Sitharaman B (2013b) Cell specific cytotoxicity and uptake of graphene nanoribbons. *Biomaterials* 34:283–293
- Dai YJ, Jia YF, Chen N, Bian WP, Li QK, Ma YB, Chen YL, Pei DS (2014) Zebrafish as a model system to study toxicology. *Environ Toxicol Chem* 33:11–17
- Defterali C, Verdejo R, Majeed S, Boschetti-de-Fierro A, Méndez-Gómez HR, Díaz-Guerra E, Fierro D, Buhr K, Abetz C, Martínez-Murillo R, Daniela Vuluga D, Alexandre M, Thomassin JM, Detrembleur C, Jérôme C, Abetz V, López-Manchado MA, Vicario-Abejón C (2016a) *In vitro* evaluation of biocompatibility of uncoated thermally reduced graphene and carbon nanotube-loaded PVDF membranes with adult neural stem cell-derived neurons and glia. *Front Bioeng Biotechnol* 4:94
- Defterali C, Verdejo R, Peponi L, Martín ED, Martínez-Murillo ER, López Manchado MA, Vicario-Abejón C (2016b) Thermally reduced graphene is a permissive material for neurons and astrocytes and de novo neurogenesis in the adult olfactory bulb *in vivo*. *Biomaterials* 82:84–93
- Dziewiecka M, Karpeta-Kaczmarek J, Augustyniak M, Majchrzycki L, Augustyniak-Jablokow MA (2016) Evaluation of *in vivo* graphene oxide toxicity for *Acheta domestica* in relation to nanomaterial purity and time passed from the exposure. *J Hazard Mater* 305:30–40
- Ersahin T, Tuncbag N, Cetin-Atalay R (2015) The PI3K/AKT/mTOR interactive pathway. *Mol Biosyst* 11:1946–1954
- Fernandes AL, Nascimento JP, Santos AP, Furtado CA, Romano LA, da Rosa CA, Monserrat JM, Ventura-Lima J (2018) Assessment of the effects of graphene exposure in *Danio rerio*: a molecular, biochemical and histological approach to investigating mechanisms of toxicity. *Chemosphere* 210:458–466
- Giese B, Klaessig F, Park B, Ralf K, Steinfeldt M, Wigger H, Gleich A, Gottschalk F (2018) Risks, release and concentrations of engineered nanomaterial in the environment. *Sci Rep* 8:1565
- Guo X, Mei N (2014) Assessment of the toxic potential of graphene family nanomaterials. *J Food Drug Anal* 22:105–115
- He JH, Guo SF, Zhu F, Zhu JJ, Chen YX, Huang CJ, Gao JM, Dong QX, Xuan YX, Li CQ (2013) A zebrafish phenotypic assay for assessing drug induced hepatotoxicity. *J Pharmacol Toxicol Methods* 67:25–32
- He K, Chen G, Zeng G, Peng M, Huang Z, Shi J, Huang T (2017) Stability, transport and ecosystem effects of graphene in water and soil environments. *Nanoscale* 9:5370–5388
- Jasim DA, Boutin H, Fairclough M, Ménard-Moyon C, Prenant C, Bianco A, Kostarelos K (2016) Thickness of functionalized graphene oxide sheets plays critical role in tissue accumulation and urinary excretion: a pilot PET/CT study. *Appl Mater Today* 4:24–30
- Kanungo J, Lantz S, Paule MG (2011) *In vivo* imaging and quantitative analysis of changes in axon length using transgenic zebrafish embryos. *Neurotoxicol Teratol* 33:618–623
- Khan I, Saeed K, Khan I (2019) Nanoparticles: properties, applications and toxicities. *Arab J Chem* 7:908–931
- Kurantowicz N, Strojny B, Sawosz E, Jaworski S, Kutwin M, Grodzik M, Wierzbicki M, Lipińska L, Mitura K, Chwalibog A (2015) Biodistribution of a high dose of diamond, graphite, and graphene oxide nanoparticles after multiple intraperitoneal injections in rats. *Nanoscale Res Lett* 10:398
- Li S, Pan X, Wallis LK, Fan Z, Chen Z, Diamond SA (2014) Comparison of TiO₂ nanoparticle and graphene-TiO₂ nanoparticle composite phototoxicity to *Daphnia magna* and *Oryzias latipes*. *Chemosphere* 12:62–69
- Lim MH, Jeung IC, Jeong J, Yoon SJ, Lee SH, Park J, Kang YS, Lee H, Park YJ, Lee HG, Lee SJ, Han BS, Song NW, Lee SC, Kim JS, Bae KH, Min JK (2016) Graphene oxide induces apoptotic cell death in endothelial cells by activating autophagy via calcium-dependent phosphorylation of c-Jun N-terminal kinases. *Acta Biomater* 46:191–203
- Lu CJ, Jiang XF, Junaid M, Ma YB, Jia PP, Wang HB, Pei DS (2017a) Graphene oxide nanosheets induce DNA damage and activate the base excision repair (BER) signaling pathway both *in vitro* and *in vivo*. *Chemosphere* 184:795–805
- Lu K, Dong S, Petersen EJ, Niu J, Chang X, Wang P, Lin S, Gao S, Mao L (2017b) Biological uptake, distribution, and depuration of radiolabeled graphene in adult zebrafish: effects of graphene size and natural organic matter. *ACS Nano* 11:2872–2885
- Manjunatha B, Park SH, Kim K, Kundapur RR, Lee SJ (2018a) *In vivo* toxicity evaluation of pristine graphene in developing zebrafish (*Danio rerio*) embryos. *Environ Sci Pollut Res Int* 25:12821–12829
- Manjunatha B, Park SH, Kim K, Kundapur RR, Lee SJ (2018b) Pristine graphene induces cardiovascular defects in zebrafish (*Danio rerio*) embryogenesis. *Environ Pollut* 243:246–254
- Meyers TR, Hendricks JD (1982) A summary of tissue lesions in aquatic animals induced by controlled exposures to environmental contaminants, chemotherapeutic agents, and potential carcinogens. *Mar Fish Rev* 44:1–17
- Modi A, Verma SK, Bellare J (2017) Graphene oxide nanosheets and d-alpha-tocopheryl ultrafiltration in polyethersulfone polyethylene glycol 1000 succinate (TPGS) doping improves biocompatibility and ultrafiltration in polyethersulfone hollow fiber membranes. *J Colloid Interface Sci* 504:86–100
- Mu S, Li G, Liang Y, Wu T, Ma D (2017) Hyper branched polyglycerol-modified graphene oxide as an efficient drug carrier with good biocompatibility. *Mater Sci Eng C Mater Biol Appl* 78:639–646
- Osterauer R, Köhler H, Triebkorn R (2010) Histopathological alterations and induction of hsp70 in ramshorn snail (*Marisa cornuarietis*) and zebrafish (*Danio rerio*) embryos after exposure to PtCl₂. *Aquat Toxicol* 99:100–107
- Ren C, Hu X, Li X, Zhou Q (2016) Ultra-trace graphene oxide in a water environment triggers Parkinson's disease-like symptoms and metabolic disturbance in zebrafish larvae. *Biomaterials* 93:83–94
- Saburi E, Islami M, Hosseinzadeh S, Moghadam AS, Mansour RN, Azadian E, Joneidi Z, Nikpoor AR, Ghadiani MH, Khodaii Z, Ardeshiryajimi A (2019) *In vitro* osteogenic differentiation

- potential of the human induced pluripotent stem cells augments when grown on graphene oxide-modified nanofibers. *Gene* 696: 72–79
- Sánchez-González S, Diban N, Bianchi F, Ye H, Urtiaga A (2018) Evidences of the effect of GO and rGO in PCL membranes on the differentiation and maturation of human neural progenitor cells. *Macromol Biosci* 18:e1800195
- Sawosz E, Jaworski S, Kutwin M, Hotowy A, Wierzbicki M, Grodzik M, Kurantowicz N, Strojny B, Lipińska L, Chwalibog A (2014) Toxicity of pristine graphene in experiments in a chicken embryo model. *Int J Nanomedicine* 9:3913–3922
- Souza JP, Baretta JF, Santos F, Paino IMM, Zucolotto V (2017) Toxicological effects of graphene oxide on adult zebrafish (*Danio rerio*). *Aquat Toxicol* 186:11–18
- Strojny B, Sawosz E, Grodzik M, Jaworski S, Szczepaniak J, Sosnowska M, Wierzbicki M, Kutwin M, Orlińska S, Chwalibog A (2018) Nanostructures of diamond, graphene oxide and graphite inhibit CYP1A2, CYP2D6 and CYP3A4 enzymes and downregulate their genes in liver cells. *Int J Nanomedicine* 13:8561–8575
- Sun J, Zhou Q, Hu X (2019) Integrating multi-omics and regular analyses identifies the molecular responses of zebrafish brains to graphene oxide: perspectives in environmental criteria. *Ecotoxicol Environ Saf* 180:269–279
- Szmidt M, Sawosz E, Urbańska K, Jaworski S, Kutwin M, Hotowy A, Wierzbicki M, Grodzik M, Lipińska L, Chwalibog A (2016) Toxicity of different forms of graphene in a chicken embryo model. *Environ Sci Pollut Res Int* 23:19940–19948
- Tabish TA, Pranjol MZI, Jabeend F, Abdullah T, Latif A, Khalid A, Ali M, Hayat H, Winyard PG, Whatmore JL, Zhang S (2018) Investigation into the toxic effects of graphene nanopores on lung cancer cells and biological tissues. *Appl Mater Today* 12:389–401
- van Leeuwen LM, Evans RJ, Jim KK, Verboom T, Fang X, Bojarczuk A, van der Sar AM (2018) A transgenic zebrafish model for the *in vivo* study of the blood and choroid plexus brain barriers using *claudin 5*. *Biol Open* 7(2):bio030494
- Vliegenthart AD, Tucker CS, Del Pozo J, Dear JW (2014) Zebrafish as model organisms for studying drug-induced liver injury. *Br J Clin Pharmacol* 78:1217–1227
- Xu M, Zhu J, Wang F, Xiong Y, Wu Y, Wang Q, Weng J, Zhang Z, Chen W, Liu S (2016) Improved in vitro and in vivo biocompatibility of graphene oxide through surface modification: poly (acrylic acid)-functionalization is superior to PEGylation. *ACS Nano* 10:3267–3281
- Zhang J, Liss M, Wolburg H, Blasig IE, Abdelilah-Seyfried S (2012) Involvement of *claudins* in zebrafish brain ventricle morphogenesis. *Ann N Y Acad Sci* 1257(1):193–198
- Zhang X, Zhou Q, Zou W, Hu X (2017) Molecular mechanisms of developmental toxicity induced by graphene oxide at predicted environmental concentrations. *Environ Sci Technol* 51:7861–7871
- Zhao Y, Wang X, Wu Q, Li Y, Wang D (2015) Translocation and neurotoxicity of CdTe quantum dots in RMEs motor neurons in nematode *Caenorhabditis elegans*. *J Hazard Mater* 283:480–489
- Zhao J, Cao XS, Wang ZY, Dai YH, Xing BS (2016) Mechanistic understanding toward the toxicity of graphene-family materials to freshwater algae. *Water Res* 111:18–27

Publisher's note Springer Nature remains neutral with regard to jurisdictional claims in published maps and institutional affiliations.